Hue University Journal of Science: Natural Science
Vol. 132, No. 1B, 93–100, 2023

pISSN 1859-1388
eISSN 2615-9678

Energy Transfer Phenomenon and Color-Tunable Properties of $Ca_2Al_2SiO_7$: Dy^{3+}/Eu^{3+} Phosphors

Do Thanh Tien[1]*, Nguyen Manh Son[2], Nguyen Dang Nhat[3], Ho Van Tuyen[4], Le Xuan Diem Ngoc[2], Tran Quoc Toan[5]

[1] University of Agriculture and Forestry, Hue University, 102 Phung Hung, Hue, Vietnam
[2] University of Sciences, Hue University, 77 Nguyen Hue, Hue, Vietnam
[3] School of Engineering and Technology, Hue University, 01 Dien Bien Phu, Hue, Vietnam
[4] Institute of Research and Development, Duy Tan University, Da Nang 550000, Vietnam
[5] Phan Boi Chau High School, 24 Hung Vuong, Pleiku, Gia Lai

* Correspondence to Do Thanh Tien <dothanhtien@hueuni.edu.vn>

(*Received: 24 May 2022; Accepted: 18 October 2022*)

Abstract. $Ca_2Al_2SiO_7$ (CAS) doped with rare-earth ions: Eu^{3+}, Dy^{3+}, and Dy^{3+}/Eu^{3+} has been successfully synthesized by the solid-phase reaction method. During the process, the sample was sintered at 1280^oC within 1 hour. The energy transfer phenomenon from Dy^{3+} to Eu^{3+} was observed in the CAS matrix. Optimal doping concentrations of both rare-earth ions (Dy^{3+}, Eu^{3+}) in CAS: Dy^{3+}/Eu^{3+} were determined for both Dy^{3+} (1.5 mol%) and Eu^{3+} (1.0 mol%), respectively. In addition, the energy transfer mechanism, CIE color coordinate, and CCT color temperature of CAS: Dy^{3+}/Eu^{3+} were also presented and discussed.

Keywords: $Ca_2Al_2SiO_7$, Dy^{3+}/Eu^{3+}, energy transfer

1 Introduction

Luminescent material has brought about numerous successes in the lighting and display fields. In recent years, luminescent material on alkaline-earth aluminosilicate matrix CAS doped with rare earth or transition metal ions has attracted interest from various research groups. Thanks to its high luminescent efficiency, spectral characteristics, and suitability for many applications. In 1992, aiming to conduct research to invent material for the laser diode, Larry and collaborators issued a publication on CAS material doped with Cr^{4+} transition metal [1]. Then, studies on the luminescent properties of CAS material doped or co-doped with RE^{3+} ions (Eu^{3+}, Er^{3+}, Ce^{3+}, Tb^{3+}, etc) have been conducted [2-6]. In particular, research on absorption transition and emission of Er^{3+} in CAS: Er^{3+} for diode laser application [3]; research on emission color manipulation and emission intensity enhancement in CAS material co-doped with Tb^{3+}, Bi^{3+} or Sm^{3+}, La^{3+} [7]; research on Energy transfer (ET) between Ce^{3+} and Tb^{3+} [5], Ce^{3+} and Mn^{2+} [8], Tm^{3+} and Dy^{3+} [9] have already been done. Therefore, we hope that the energy transfer phenomenon between Dy^{3+} and Eu^{3+} also occurs in CAS: Dy^{3+}/Eu^{3+}. For that reason, the paper has two purposes: (1) Study the energy transfer between two rare earth metal ions: Dy^{3+} and Eu^{3+} in CAS matrix. (2) Study the CIE color coordinate and CCT color temperature of CAS: Dy^{3+}/Eu^{3+}. In addition, the phase structure and luminescent characteristics of single-doped CAS: Dy^{3+} and Eu^{3+} materials are also presented and discussed.

2 Experimental

Eu^{3+} and Dy^{3+} ions doped with CAS phosphor were prepared by the solid-state reaction. Chemical reagents include $CaCO_3$ (99.9%, China), Al_2O_3 (99%, China), SiO_2 (99.9%, Korea), Eu_2O_3 (99.9%, Merck), and Dy_2O_3 (99.9%, Merck). These precursors are weighted by molar ratio and mixed with 4 *weight* percent B_2O_3 (used as fluxing agents). The mixtures are well ground for two hours using an agate mortar. Then the mixtures were annealed at 1280°C for 1 hour [10]. Experimental measurements such as X-ray diffraction (XRD), photoluminescence (PL), Photoluminescence excitation (PLE), and color chromaticity coordinates (CIE) were made in order to study the structural characteristic and luminescent properties of the prepared samples. XRD patterns were recorded using an x-ray diffractometer (D8Advance; Bruker, Germany). PL and PLE spectra were examined using a spectrophotometer (FL3-22; Horiba Jobin-Yvon) at room temperature.

3 Results and Discussion

3.1 Crystal structure of single-doped and co-doped CAS: Dy^{3+}/Eu^{3+}

The crystal structure of $Ca_2Al_2SiO_7$ doped with rare-earth ions and luminescent material was characterized by the X-ray diffraction method. XRD diagrams of $Ca_2Al_2SiO_7$: Dy^{3+} (x mol%) and Eu^{3+} (1.0 mol%) are shown in Figure 1. The analysis results indicate that the material had the desired $Ca_2Al_2SiO_7$ phase structure, P-42$_1$m space group, and tetragonal phase, well in accordance with the JCPDS 35-0755 standard card. The phase structure of $Ca_2Al_2SiO_7$ had high repetitiveness when the concentration of Dy^{3+} dopant was increased from 0 mol% to 3.5 mol%, indicating that the technological procedure has high stability and repetitiveness. On the other hand, the XRD diagram shows no characteristic peaks of rare-earth ions or other initial reagents. The observation proves that the small doping concentration in the matrix does not change the material's phase structure [11].

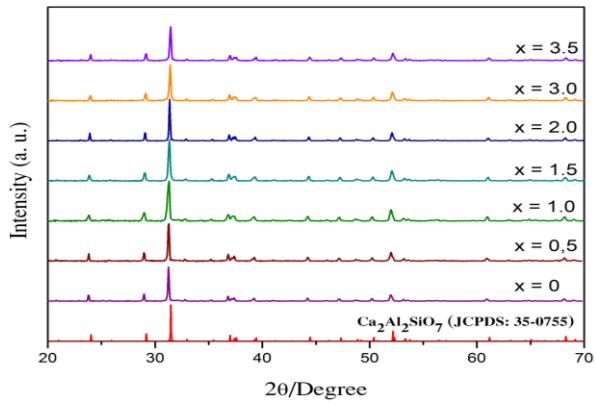

Fig. 1. The XRD diagram of CAS: Dy^{3+} (x mol%), Eu^{3+} (1.0 mol%)

3.2 Luminescent properties of $Ca_2Al_2SiO_7$: Dy^{3+}/Eu^{3+} phosphor

Energy transfer phenomena from Dy^{3+} to Eu^{3+} have also been detected in other matrices such as $NaLa(MoO_4)_2$ [12], $Ca_2ZnSi_2O_7$ [13], and Gd_2MoO_6 [14]. We expected that the energy transfer phenomenon from Dy^{3+} to Eu^{3+} would also occurs in the CAS matrix. To determine whether ET occurs in ET or not, the following spectral characteristics were investigated: The PL spectrum of CAS: Dy^{3+} (0.5 mol%) and the PLE spectrum of CAS: Eu^{3+} (0.5 mol%) are shown in Figure 2.

The results show that the PL spectrum of Dy^{3+} overlapped with the excitation maxima of Eu^{3+} in the region from 400 to 600 nm. Notably, the relatively strong excitation emission located at 463 nm of Eu^{3+} ($^7F_0 \rightarrow {}^5D_2$) is totally within the emission band of Dy^{3+}. Therefore, we predicted that ET from Dy^{3+} to Eu^{3+} could occur in the CAS matrix.

pISSN 1859-1388
eISSN 2615-9678

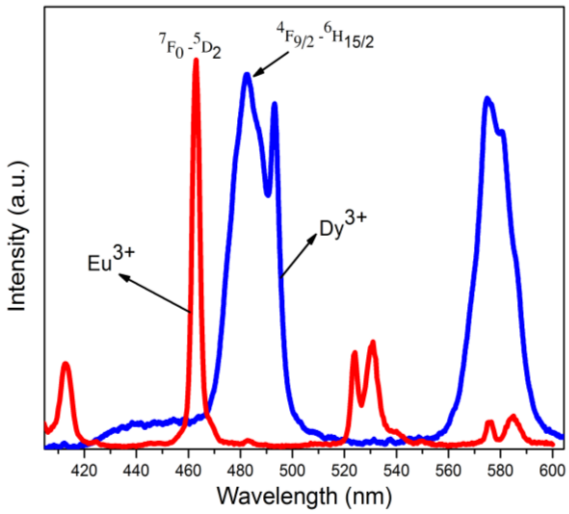

Fig. 3. PLE spectra of CAS: Eu^{3+} (0.5 mol%) (λ_{em} = 617 nm) and PL spectra of CAS: Dy^{3+} (0.5 mol%) λ_{ex}=350 nm.

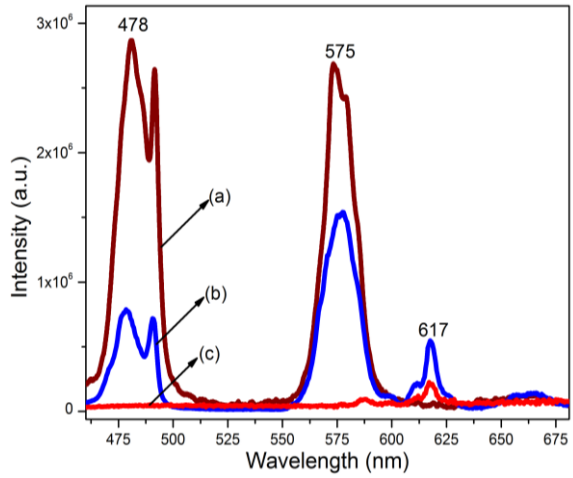

Fig. 2. PL spectra of CAS: Dy^{3+} (0.5 mol%) (a), PL spectra of CAS: Dy^{3+} (0.5 mol%), Eu^{3+} (1.0 mol%) (b) and PL spectra of CAS: Eu^{3+} (1.0 mol%) (c), λ_{ex}=350 nm

PL spectra of CAS samples single or co-doped with Dy^{3+} and Eu^{3+} are shown in Figure 3. Both spectra were excited at a wavelength of 350 nm, taken at room temperature, in the same conditions. The spectra show that, when excited at a wavelength of 350 nm, the PL spectrum of CAS: Eu^{3+} has some narrow lines, the line at 617 nm has the highest intensity, corresponding to $^5D_0 \rightarrow {}^7F_2$ of Eu^{3+} ions [15-17]. However, the luminescent intensity of Eu^{3+} in CAS: Eu^{3+} is weaker than that of CAS: Dy^{3+}. The PL spectrum of CAS: Dy^{3+} has narrow lines located at 478 and 575 nm, which are the characteristic transition and emission of Dy^{3+} [18, 19], correspond to $^4F_{9/2} \rightarrow {}^6H_J$ (J = 15/2, 13/2) transitions, and have a stronger intensity than that of CAS: Eu^{3+}. The spectrum of CAS:Eu^{3+} material shows characteristic emission of both Dy^{3+} and Eu^{3+}, including narrow lines located at 478 and 575 nm, which correspond to the transition of Dy^{3+}, and a maximum located at 617 nm, which corresponds to the transition of Eu^{3+} [20]. However, the intensity of lines at 478 and 575 nm in co-doped samples is considerably smaller than that of Dy^{3+} single-doped samples. Meanwhile, the maximum emission intensity of lines corresponding to Eu^{3+} increased considerably compared to that of CAS: Eu^{3+} with the same dopant concentration. The observation shows that energy transfer from Dy^{3+} to Eu^{3+} could occur in the CAS matrix.

The PLE spectra of CAS: Eu^{3+} (1,0 mol%), excited at a wavelength of 617 nm; CAS: Dy^{3+} (0,5 mol%), excited at a wavelength of 575 nm and CAS: Eu^{3+} (1,0 mol%); and Dy^{3+} (0,5 mol%), excited at a wavelength of 617 nm are shown in Figure 4. The spectrum shows that the excitation transition of Eu^{3+} that causes the characteristic peak of Eu^{3+} in CAS: Eu^{3+} has low intensity, narrow lines with maxima located at 360, 374, 380, 393, and 412 nm. Besides, the PLE spectrum of CAS: Dy^{3+} has high intensity, narrow lines with maxima located at 322, 350, 363, 383, 425, and 451 nm. Meanwhile, the PLE spectrum of CAS: Dy^{3+}/Eu^{3+} corresponds to a peak at 617 nm of Eu^{3+} and has a similar shape to the PLE spectrum of Eu^{3+} , plus a few minor transitions due to the contribution of Dy^{3+}. The contribution to the direct stimulation of Eu^{3+} is very small, mainly due to the absorption of Dy^{3+} ions, to generate emission of Dy^{3+} through ET between Dy^{3+} and Eu^{3+}. The observation shows that the emission efficiency of Eu^{3+} is relatively high when co-doped with Dr^{3+} in the CAS matrix.

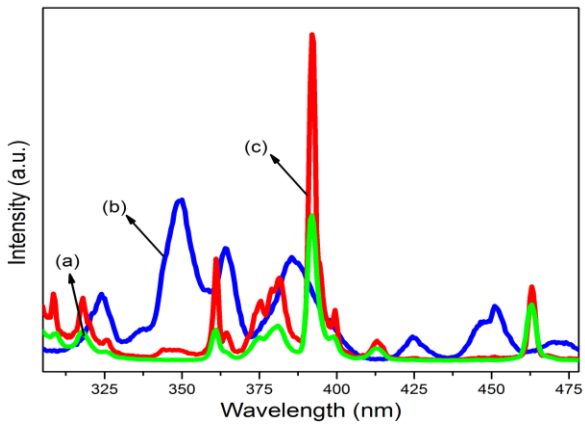

Fig. 4. PLE spectra of CAS: Eu^{3+} (1.0 mol%) with (λ_{em} = 617 nm) (a), CAS: Dy^{3+} (0.5 mol%) with (λ_{em} = 575 nm) (b), CAS: Dy^{3+} (0.5 mol%), Eu^{3+} (1.0 mol%) with (λ_{em} = 617 nm) (c)

To further clarify the ET mechanism from Dy^{3+} to Eu^{3+} in CAS: Dy^{3+}/Eu^{3+}, we studied the PL spectra of the CAS: Dy^{3+} (x mol%), and Eu^{3+} (1.0 mol%), stimulated at 350 nm. All spectra were taken at room temperature with the same measuring conditions (Figure 5). The result shows that, when the sample is not co-doped with Dy^{3+}, the emission intensity of CAS: Eu^{3+} is very weak, and only characteristic emission of Eu^{3+} in the matrix is observed. As the doping concentration of Dy^{3+} increased from 0,5 – 3,5 mol%, the position of the emission maximum of both Eu^{3+} and Dy^{3+} in the PL spectrum remained unchanged, while the emission intensity of both ions increased. The phenomenon showed that, although the concentration of Eu^{3+} ions remained unchanged, their emission intensity increased as the doping concentration of Dy^{3+} increased. The result further confirmed the occurrence of ET from Dy^{3+} to Eu^{3+} ions in the CAS matrix. Besides, Figure 6 shows the PLE spectra of CAS: Dy^{3+} (x mol%), Eu^{3+} (1.0 mol%) excited at a wavelength of 617 nm. As the doping concentration of Dy^{3+} increased, the shape of the PLE spectra remained unchanged, but the emission intensity changed. The PLE spectra of the co-dope sample still have a peak at 350 nm, which corresponds to the absorption of Dy^{3+} ions.

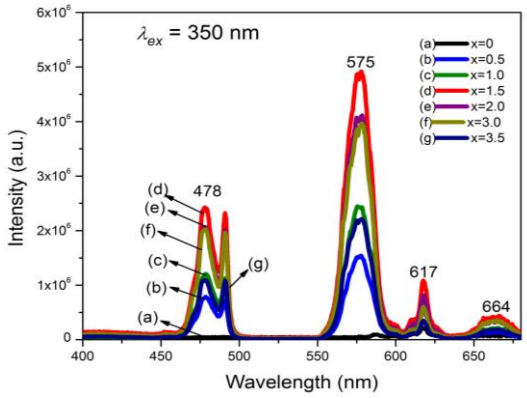

Fig. 5. PL Spectra of CAS: Dy^{3+} (x mol%), Eu^{3+} (1.0 mol%), λ_{ex} = 350 nm

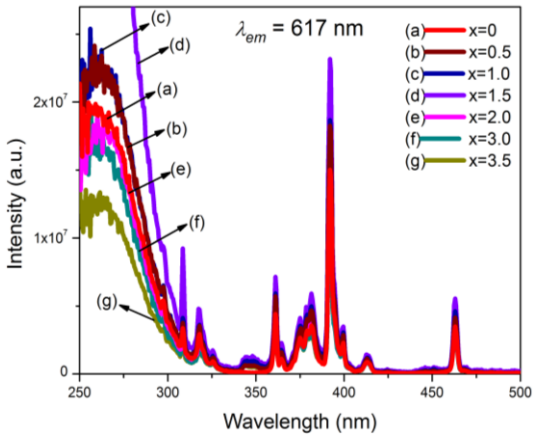

Fig. 6. PLE Spectra of CAS: Dy^{3+} (x mol%), Eu^{3+} (1.0 mol%), λ_{em} = 617 nm

The mechanism of energy transfer from Dy^{3+} to Eu^{3+} ions in the CAS matrix is shown in Figure 7, based on the energy diagram of Dy^{3+} and Eu^{3+} ions. When being stimulated by a wavelength of 350 nm, electrons of Dy^{3+} transit from the $^6H_{15/2}$ ground state to the $^6P_{7/2}$ excited state, then electrons transit to the lowest excited state $^4F_{9/2}$ of Dy^{3+}, before transiting to the ^6H_J ground state (with J = 15/2, 13/2, 11/2), emitting narrow lines with maxima located at 478, 575, and 664 nm. Simultaneously, part of the excitation energy of Dy^{3+} is transferred to Eu^{3+}, causing it to transit to an excited state followed by a non-emission to $^5D_0$ low excited states before transiting to ^7F_J ground state, emitting narrowly lined characteristics peaks of Eu^{3+}.

pISSN 1859-1388
eISSN 2615-9678

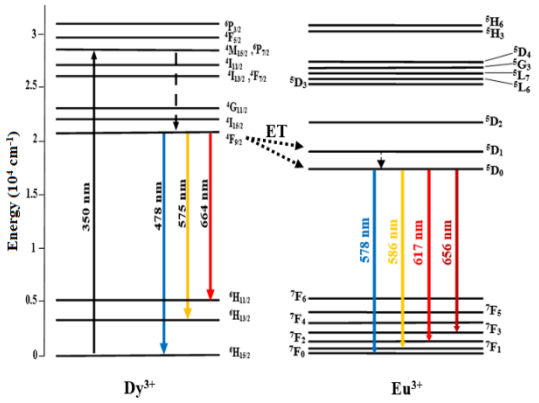

Fig. 7. Energy transfer mechanism from Dy^{3+} ion to Eu^{3+} ion in CAS

In order to study the influence of energy transfer from Dy^{3+} to Eu^{3+} in the CAS matrix, the dependence of the intensity of characteristic emission of Dy^{3+} and Eu^{3+} ions in CAS: Dy^{3+} (x mol%) and Eu^{3+} (1,0 mol%) samples on the doping concentration of Dy^{3+} ions is shown in Figure 8. The result shows that the emission intensity corresponds to the wavelengths 478 and 575 nm of Dy^{3+} and 617 nm of Eu^{3+} and increases when the doping concentration of Dy^{3+} increases, reaching its maximum when the doping concentration of Dy^{3+} reaches 1.5%/mol. Beyond this value, the maximum luminescent intensity of both Dy^{3+} and Eu^{3+} decreases, the decrease is because of the concentration quenching phenomenon.

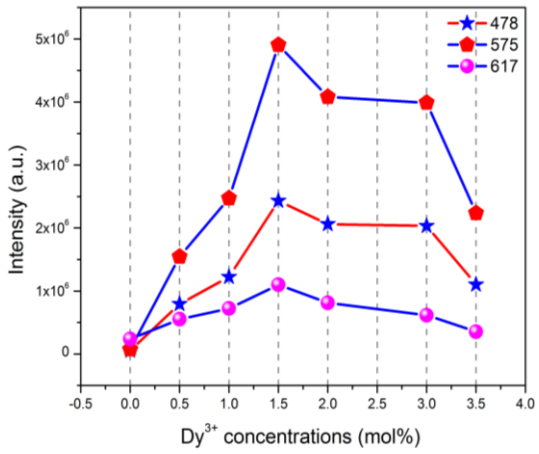

Fig. 8. The dependence of PL intensity (peak at 478 nm, 575 nm and 617 nm) on the concentration of Dy^{3+} ion

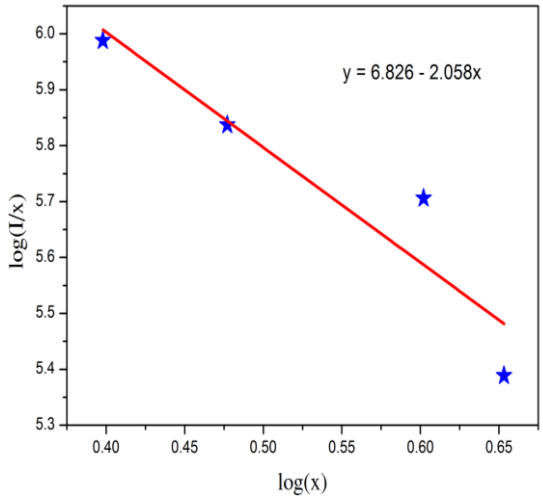

Fig. 9. The relation between *log(I/x)* and *log(x)* of CAS: Dy^{3+}/Eu^{3+}

According to the theory of dopant concentration quenching of Dexter and Blasse, the concentration quenching ET critical distance between Dy^{3+} and Eu^{3+} is given by the following equation (1) [21-23].

$$R_c = 2\left(\frac{3V}{4\pi x_c N}\right)^{1/3}, \quad (1)$$

where x_c is the total concentration of Dy^{3+} and Eu^{3+} ions at which the quenching begins to occur, N is the number of cations in an unit cell, V is the volume of the unit cell. From the PL spectral data of CAS: Dy^{3+} (x mol%) and Eu^{3+} (1.0 mol%), we have calculated and determined that V= *299.39* Å^3, N = 2 [6], and the concentration at which the intensity quenching begins to occur is Eu^{3+} = 1.0 mol% and Dy^{3+} = 1.5 mol% in CAS: Dy^{3+}/Eu^{3+}. Substituting these values to equation (1), we obtain the ET critical distance between Dy^{3+} and Eu^{3+} was 22.53 Å. The distance is rather large, therefore, the luminescent intensity concentration quenching caused by multipolar interaction is used to explain the phenomenon in material containing two type's emission center. The graphs of *log(I/x)* with *log(x)* of CAS: Dy^{3+}/Eu^{3+} correspond to different concentrations of Dy^{3+} and are shown in Figure 9. From the graph, the slope for CAS:

Dy^{3+}/Eu^{3+} is determined to be -2.058 and Q is calculated to be 6.174, very close to 6. The result showed that d-d interaction is the main contributor to luminescent intensity dopant concentration quenching of Dy^{3+} and Eu^{3+} in CAS: Dy^{3+}/Eu^{3+}.

3.3 Color chromaticity coordinates of CAS: Dy^{3+}/Eu^{3+} phosphors

As we know, CIE color coordinates are usually used to assess the particular applicability of luminescent material [24-27]. For CAS: Dy^{3+}/Eu^{3+}, stimulated at 350 nm, the color coordinate value of CAS: Dy^{3+}/Eu^{3+} could be changed by adjusting the concentration of Dy^{3+}. The color coordinate of CAS: Eu^{3+} (1.0 mol%) is in the red region, while that of CAS: Dy^{3+} (0.5 mol%) is in the whitish yellow region. The co-doping of Dy^{3+} with CAS: Eu^{3+} causes a color coordinate shift toward the orange direction (Figure 10).

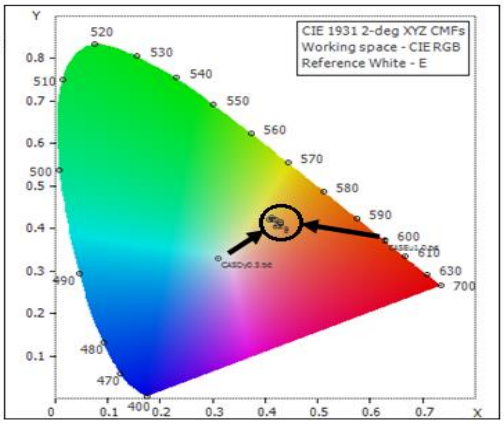

Fig. 10. CIE Color coordinate of the CAS: Dy^{3+} (x mol%), Eu^{3+} (1.0 mol%) samples when being stimulated by a wavelength at 350 nm

3.4 Correlated color temperature of CAS: Dy^{3+}/Eu^{3+} phosphors

The calculated CIE (the Commission International de l'Eclairage) chromaticity coordinates of CAS: Dy^{3+}/Eu^{3+} phosphors from the emission spectra are shown in Fig. 10. The x and y color chromaticity coordinates of CAS: Dy^{3+}/Eu^{3+} phosphors were used to calculate the correlated color temperature (CCT) by using McCamy's relation [24-26].

$$CCT = -449n^3 + 3525n^2 - 6823n + 5520.33, \quad (2)$$

where n = $(x - x_e)/(y - y_e)$ is the inverse slope line and (x_e = 0.332, y_e = 0.186) indicates the isotemperature lines' epicenter [25]. The color chromaticity coordinates and CCT values of CAS: Dy^{3+}/Eu^{3+} phosphors with various Dy^{3+}/Eu^{3+} ions concentrations are listed in Table I. The results from Fig. 10 and Table I show that the color chromaticity coordinates are in the red region and have slight differences with various Dy^{3+}/Eu^{3+} ions concentrations. The CCT values of the prepared samples increase slightly as Dy^{3+} concentrations increase, and their temperature corresponds to 'Warm White' light in human visual perception [28].

Table 1. Color chromaticity coordinates (x, y) and CCT of CAS: Dy^{3+}/Eu^{3+} materials.

Samples	x	y	CCT (K)
CAS: Eu^{3+} (1.0 mol%)	0.629	0.370	1803
CAS: Dy^{3+} (0.5 mol%)	0.311	0.330	6591
CAS: Dy^{3+} (0.5 mol%), Eu^{3+} (1.0 mol%)	0.429	0.412	3206
CAS: Dy^{3+} (1.0 mol%), Eu^{3+} (1.0 mol%)	0.430	0.416	3218
CAS: Dy^{3+} (1.5 mol%), Eu^{3+} (1.0 mol%)	0.418	0.420	3467
CAS: Dy^{3+} (2.0 mol%), Eu^{3+} (1.0 mol%)	0.415	0.421	3530
CAS: Dy^{3+} (3.0 mol%), Eu^{3+} (1.0 mol%)	0.407	0.421	3687
CAS: Dy^{3+} (3.5 mol%), Eu^{3+} (1.0 mol%)	0.412	0.427	3627

pISSN 1859-1388
eISSN 2615-9678

4 Conclusions

Studying the PL and PLE spectra of CAS: (x mol%) Dy^{3+}, (1.0 mol%) Eu^{3+}, samples with x = 0; 0.5; 1.0; 1.5; 2.0; 3.0; 3.5, we found out that the optimal doping concentration of Dy^{3+} was 1,5mol%, at which the maximum luminescent intensity was obtained. In addition, energy transfer from Dy^{3+} to Eu^{3+} phenomenon was observed in the CAS matrix; d-d interaction is the main contributor to luminescent intensity dopant concentration quenching of Dy^{3+} and Eu^{3+} in CAS: Dy^{3+}/Eu^{3+}. Luminescent color temperature of CAS: Dy^{3+}/Eu^{3+} co-doped material when excited at a wavelength of 350 nm was within 3200 - 3700K; the CIE color coordinate shows that the material emitted orange radiation, suitable for developing LED in lighting technology.

Acknowledgment

This study was supported by Hue University under grant number DHH2021-02-154.

References

1. Laary DM, Toomas HA, Bruce HTC. Crystal growth and spectroscopic properties of Cr^{4+} in $Ca_2Al_2SiO_7$ and $Ca_2Ga_2SiO_7$. Optical Material. 1992;1(2):91-100.
2. Akiyama M, Xu CN, Nonaka K. Improvement in Mechanoluminescence Intensity of $Ca_2Al_2SiO_7$: Ce by the Statistical Approach. Journal of The Electrochemical Society. 2003;150(5):H115-H118.
3. Boulanger PL, Doualan JL, Girard S, Margerie J, Moncorgé R, Viana B. Excited-state absorption of Er^{3+} in the $Ca_2Al_2SiO_7$ laser crystal. Journal of Luminescence. 2000;86:15-21.
4. Tiwari G, Brahme N, Sharma R, Bisen DP, Sao SK, Kurrey UK. Enhanced long-persistence of $Ca_2Al_2SiO_7$: Ce^{3+} phosphors for mechanoluminescence and thermoluminescence dosimetry. Journal of Materials Science: Materials in Electronics. 2016;27:6399-6407.
5. Jiao H, Wang Y. $Ca_2Al_2SiO_7$: Ce^{3+}, Tb^{3+}: A White-Light Phosphor Suitable for White-Light-Emitting Diodes. Journal of The Electrochemical Society. 2009;156(5):J117-J120.
6. Zhang Q, Wang J, Zhang M, Ding W, Su Q. Enhanced photoluminescence of $Ca_2Al_2SiO_7$: Eu^{3+} by charge compensation method. Applied Physics Letters. 2007;88:805-809.
7. Pawade VB, Kohale RL, Ovhal DA, Dhoble NS, Dhoble SJ. Intense green-red-emitting Tb^{3+}, Tb^{3+}/Bi^{3+}-doped and Sm^{3+}, Sm^{3+}/La^{3+}-doped $Ca_2Al_2SiO_7$ phosphors. Luminescence. 2020;1:1-7.
8. Teixeira VC, Montes PJR, Valerio MEG. Structural and optical characterizations of $Ca_2Al_2SiO_7$: Ce^{3+}, Mn^{2+} nanoparticles produced via a hybrid route. Optical Materials. 2014;36(9):1580-1590.
9. Abudouwufu T, Sambasivam S, Wan Y, Abudoureyimu A, Yusufu T, Tuxun H, et al. Energy Transfer Behavior and Color-Tunable Properties of $Ca_2Al_2SiO_7$: RE^{3+} (RE^{3+} = Tm^{3+}, Dy^{3+}, Tm^{3+}/Dy^{3+}) for White-Emitting Phosphors. Journal of Electronic Materials. 2018.
10. Tien DT, Son NM. Preparation and spectroscopic properties of $Ca_2Al_2SiO_7$: Tb^{3+} phosphor. Hue University Journal of Science: Natural Science. 2019;128(1B):5-10.
11. Yang P, Yu X, Yu H, Jiang T, Xu X, Yang Z, et al. $Ca_2Al_2SiO_7$: Bi^{3+}, Eu^{3+}, Tb^{3+}: Apotential single-phased tunable-color-emitting phosphor. Journal of Luminescence. 2013;135:206-210.
12. Du P, Yu JS. Energy transfer mechanism and color controllable luminescence in Dy^{3+}/Eu^{3+}-codoped $NaLa(MoO_4)_2$ phosphors. Journal of Alloys and Compounds. 2015;653:468-473.
13. Mondal K, Manam J. Investigation of photoluminescence properties, thermal stability, energy transfer mechanisms and quantum efficiency of Ca 2 ZnSi 2 O 7 : Dy 3+ , Eu 3+ phosphors. Journal of Luminescence. 2018;195:259-270.
14. Dutta S, Sharma SK. Energy transfer between Dy^{3+} and Eu^{3+} in Dy^{3+}/Eu^{3+}-codoped Gd_2MoO_6. Journal of Materials Science. 2016;51(14):6750-6760.
15. Chuai XH, Zhang HJ, Li FS, Chou KC. The luminescence of Eu^{3+} ion in $Ca_2Al_2SiO_7$. Optical Materials. 2004;25(3):301-305.
16. Grzyb T, Runowski M, Lis S. Facile synthesis, structural and spectroscopic properties of GdF_3: Ce^{3+}, Ln^{3+} (Ln^{3+}= Sm^{3+}, Eu^{3+}, Tb^{3+}, Dy^{3+}) nanocrystals with bright multicolor luminescence. Journal of Luminescence. 2014;154:479-486.

17. Li M, Wang L, Ran W, Deng Z, Shi J, Ren C. Tunable Luminescence in $Sr_2MgSi_2O_7$: Tb^{3+}, Eu^{3+} Phosphors Based on Energy Transfer. Materials (Basel). 2017 Feb 24;10(227):1-11.

18. Lakshminarayana G, Baki SO, Lira A, Kityk IV, Caldiño U, Kaky KM, et al. Structural, thermal and optical investigations of Dy^{3+}-doped B_2O_3-WO_3-ZnO-Li_2O-Na_2O glasses for warm white light emitting applications. Journal of Luminescence. 2017;186:283-300.

19. Wang L, Xu M, Zhao H, Jia D. Luminescence, energy transfer and tunable color of Ce^{3+}, Dy^{3+}/Tb^{3+} doped $BaZn_2(PO_4)_2$ phosphors. New Journal of Chemistry. 2016;40(4):3086-3093.

20. Li K, Shang M, Lian H, Lin J. Recent development in phosphors with different emitting colors via energy transfer. Journal of Materials Chemistry C. 2016;4(24):5507-5530.

21. Kaur S, Rao AS, Jayasimhadri M. Color tunability and energy transfer studies of Dy^{3+}/Eu^{3+} co-doped calcium aluminozincate phosphor for lighting applications. Materials Research Bulletin. 2019;116:79-88.

22. Li G, Li M, Li L, Yu H, Zou H, Zou L, et al. Luminescent properties of $Sr_2Al_2SiO_7$: Ce^{3+}, Eu^{2+} phosphors for near UV-excited white light-emitting diodes. Materials Letters. 2011;65:3418-3420.

23. Tien DT, Manh Son N, Tuat LV, Liem LN. Energy Transfer between Ce^{3+}-Dy^{3+} in $Ca_2Al_2SiO_7$: Ce^{3+}, Dy^{3+} Phosphor. IOP Conf Series: Materials Science and Engineering. 2018;540 012001-012006.

24. Van Do P, Quang VX, Thanh LD, Tuyen VP, Ca NX, Hoa VX, et al. Energy transfer and white light emission of $KGdF_4$ polycrystalline co-doped with Tb^{3+}/Sm^{3+} ions. Optical Materials. 2019;92:174-180.

25. Lakshminarayana G, Baki SO, Lira A, Caldiño U, Meza-Rocha AN, Kityk IV, et al. Effect of alkali/mixed alkali metal ions on the thermal and spectral characteristics of Dy^{3+}: B_2O_3-PbO-Al_2O_3-ZnO glasses. Journal of Non-Crystalline Solids. 2018;481:191-201.

26. McCamy CS. Correlated Color Temperature as an Explicit Function of Chromaticity Coordinates. Color research and application. 1992;17(2):142-144.

27. Tuyen VP, Quang VX, Van Do P, Thanh LD, Ca NX, Hoa VX, et al. An in-depth study of the Judd-Ofelt analysis, spectroscopic properties and energy transfer of Dy^{3+} in alumino-lithium-telluroborate glasses. Journal of Luminescence. 2019;210:435-443.

28. Choudhury AKR. Characteristics of light sources. Principles of Colour and Appearance Measurement 2014.